# *Final Draft*
## of the original manuscript:

Bohne, Y.; Manova, D.; Blawert, C.; Stoermer, M.; Dietzel, W.; Maendl, S.:

**Influence of ion energy on morphology and corrosion properties
of Mg alloys formed by energetic PVD processes**

# INFLUENCE OF ION ENERGY ON MORPHOLOGY AND CORROSION PROPERTIES OF Mg ALLOYS FORMED BY ENERGETIC PVD PROCESSES

**Y. Bohne[1], D. Manova[1], C. Blawert[2], M. Störmer[2], W. Dietzel[2], S. Mändl[1][*],**

[1]*Leibniz-Institut für Oberflächenmodifizierung, Leipzig, Germany*

[2]*Center for Magnesium Technology, GKSS Forschungszentrum Geesthacht, Germany*

## Abstract

Different PVD processes − magnetron sputtering, ion beam sputtering and vacuum arc deposition − are used to produce novel corrosion resistant Mg alloys with the average energy per deposited atom increasing from 5 − 10 to 15 − 45 eV. Correspondingly, a transition from a 3-dimensional columnar growth regime towards a layer-by-layer growth at increased energies was observed with the film texture changing from a weak basal texture towards a highly oriented film with the c-axis normal to the surface. Additionally, a higher energy helped stabilizing supersaturation, especially for Mg-Ti alloys. However, only a weak influence of the morphology on the corrosion rates was observed, which were mainly governed by the chemical composition of the films.

[*] Corresponding Author:
Leibniz-Institut für Oberflächenmodifizierung, Permoserstr. 15, 04318 Leipzig, Germany
Tel: +49 341 235 2944, Fax: + 49 341 235 2313, E-mail: stephan.maendl@iom-leipzig.de

## 1. Introduction

Physical vapour deposition (PVD) is an established technology to obtained individually tailored surface coatings on various substrates. One of the most important parameters is the average energy per incoming particle where higher values lead to an increased surface mobility [1,2]. Additionally, changes in the surface morphology and texture are observed with higher energies leading to films with larger grains and less defects while the momentum of the incoming particles can align or orientate the growing crystallites [3,4].

Magnesium is an attractive material for transport applications as automotive and aerospace, primarily of its light weight [5,6]. Mg alloys have the highest strength-to-weight-ratio of all the structural metals [7,8]. However, several drawbacks, among them a relatively poor corrosion resistance, restrict the application of unprotected magnesium alloys [9,10]. Consequently, corrosion protection is of great importance. In this presentation, the influence of PVD process parameters on selected binary and ternary Mg-based corrosion protective coatings are investigated. The investigated PVD processes include magnetron sputtering (MS), ion beam sputtering (IBS) and vacuum arc deposition (VAD).

## 2. Experiment

Table 1 shows a summary of the different PVD processes used for these investigations. Magnetron sputtering sources were used to prepare pure Mg-films with a thickness of about 3 $\mu$m, at a source power of about 160 W and an argon gas pressure of 0.2 Pa. The base pressure of the ultra-high vacuum chamber was below $10^{-5}$ Pa. The sputtering gas used was high purity argon gas (7.0). The samples were coated under an angle of about 25° to the substrate normal. The target-to-source distance was about 15 cm, resulting in a deposition rate of approximately 3 – 4 $\mu$m/h at average particle energies of 5 – 10 eV.

The ion beam sputtering experiments were performed in an UHV chamber using Argon ions from 800 to 1200 eV [11]. The angle between the ion source and the substrate normal

was 45º with the target normal dividing this angle into two equal parts. The respective distances were 15 cm. Beside sputtered atoms with a kinetic energy between 1 and 5 eV, high energy backscattered Ar ions were impinging on the substrate during the film deposition, yielding an average ion energy of 8 − 15 eV per deposited particle. VAD was either used in conjunction with IBS or as a stand-alone process. At a total current of 100 A, an ion current of about 10 could be extracted from the cathode. Using appropriate filtering techniques, macroparticles emitted from the cathode were suppressed at the expense of a reduced ion current. Average energies of 15 − 45 eV were typical for the stand-alone mode while values of 10 − 25 eV can be estimated for the combination with IBS, depending on the relative ion current densities.

Beside commercially pure Mg (Mg 99.93 wt.-%, impurities: Ni, Cu, Fe, Be and Si in the ppm range), the alloy systems Mg-Al, Mg-Si, Mg-Sn, Mg-Ti, Mg-RE (Rare Earth: La, Ce, Pr, Nd), Mg-Ti-Al and Mg-Zr-Al were used as starting materials to obtain coatings on Si and Mg alloy substrates.

Scanning electron microscopy (SEM) was performed to analyze the morphology while X-ray diffraction (XRD) measurements were used to identify the phase components. Additionally, ion beam methods - Rutherford backscattering spectroscopy (RBS) and elastic recoil detection analysis (ERDA) - were employed to obtain qualitative and quantitative information on the composition of the films. Information about the general corrosion properties of the coating systems and the as-cast alloys were gathered with potentiodynamic polarization measurements. The specimens were tested in 0.5 % NaCl solution at a pH of 11 using an exposed surface area of around 0.5 cm².

## 3. Results & Discussion

Except for a thin surface layer of less than 5 nm, which is enriched with oxygen, homogeneous films were obtained with ion beam analysis in all cases [12]. Bulk contaminations with

C, H and O are below 0.5 at.%, comparable to the purity of the sputter targets. Any influences of concentration gradients or contaminations on the microstructure and the corrosion can be excluded in the present experiments.

Fig. 1 shows SEM images of the microstructure of pure Mg coatings deposited using the three different methods. For the first two processes, the hexagonal structure is still visible, while smoother surfaces with fewer visible topological structures are formed for the latter process. The total layer thickness for all these samples was about 3 μm to eliminate influences of the layer thickness on the morphology. With increasing average ion energy from MS via IBS to VAD, a transition from columnar growth to layer-by-layer growth is observed, which is in agreement with theoretical considerations originally propagated by Thornton [13]. With increasing the deposited energy per particle, a higher (transient) mobility of the atoms impinging on the surface is obtained, thus increasing the apparent surface temperature. At the same deposition rate, the higher mobility will lead to a larger diffusivity, thus allowing a transport from the original arrival site.

Small influences of the total layer thickness on the morphology cannot be ruled out, however, using similar particle fluxes and deposition times should minimize such secondary effects. It is known that with increasing thickness, a reduction of the average crystallite size is observed while smaller deposition rates improve the crystalline quality [14]. Furthermore, recrystallisation effects and tilting of the crystallites by varying the incident angle of the energetic particles are reported in the literature [15,16]. Further investigations of these effects during deposition of Mg alloys are in progress and will be published separately.

For magnesium alloys also a significant influence of the chemical composition on the morphology was observed, with all alloying elements generally remaining in solid solution and promoting layer by layer growth already at lower ion energies,. Only at very high contents of alloying elements (far beyond equilibrium solubility), decomposition of solid solution can

occur and the morphology is influenced. This phase segregation will always lead to rougher surfaces and smaller crystallites.

The high degree of preferential orientation, improving with increasing energy which could be inferred from the SEM viewgraphs was investigated with XRD in detail. Only the hexagonal Mg phase was found with no traces of additional precipitates. At the same time, a strong preferential orientation was found with the c-axis tending to align parallel to the surface normal. In accordance with the respective alloying element, a lattice contraction or expansion was observed, while additional intrinsic stress in some samples cannot be ruled out and further investigations are needed here.

All of these investigated samples have alloy contents beyond the equilibrium solubility, in some cases far beyond this limit. MgTi63 is still stable when produced by IBS+VAD with the solubility limit near 0.2 wt.%, however lower average particle energies lead to decomposition in some systems. MgTi26 by IBS is still single-phased whereas MgTi59 by IBS decomposes into α-Mg and β-Ti. For the Mg-Sn system with coatings produced by IBS, similar effects are observed starting near an Sn content of about 26 wt.% (cf. Fig. 2). The observation of higher particle energies necessary to stabilize the supersaturation is in contradiction to traditional theories where higher temperatures - or higher mobilities – should lead t a faster reversion to the thermodynamically favoured state, i.e. phase segregation. The origin of this effect is not understood at the moment.

A strong evolution of the texture was already obtained at the transition from MS to IBS. A typical Mg(101) pole-figure measured from a sample from the Mg-Al-Zr series is shown in Fig. 3 with the resolution limited by the experimental setup. The FWHM of corresponding Mg(002) rocking curves were smaller than 1° for all IBS samples from this alloys series, while much larger values were obtained for samples from MS deposition. Furthermore, besides the influence of the average energy per particle, a systematic influence of the alloy sys-

tem on the width of the rocking curves was found. It can be possible that alloy-systems with a higher tendency towards amorphous systems show a broader distribution of crystallite orientations, but further investigations are needed on this point.

The corrosion data itself show no significant influence of the process or ion energy as long as Si was used as a substrate. For metallic substrates, such as cast magnesium components, the adhesion was improved with increasing ion energy. More noble (compared to the substrate) corrosion protective layers on Mg alloys show a large tendency of galvanic corrosion via pinholes, grain boundaries or other defects associated with the respective PVD process. Fig. 4 shows an overview on the systematic variation of the corrosion behaviour as a function of the alloy composition. Especially Si and RE can be used to increase the shift of the free corrosion potential. Al is in that sense not so effective, but has the advantage that the corrosion rate can be lowered. Even more effective in lowering the corrosion rate is titanium, but it has the clear disadvantage that the free corrosion potential is shifted to more noble potentials compared to cast Mg, thus already at low Ti contents a cathodic protection will not be possible anymore.

## 4. Summary & Conclusions

Mg alloy coatings can be deposited using different PVD techniques with the corresponding morphology and texture closely related with the average energy per deposited particle according to the standard model. However, differences in the solubility limits from non-equilibrium processes are observed with higher energies favouring a larger mixing range suppressing decomposition, which cannot be explained at present. Differences in the alloy composition are the major influences affecting the corrosion properties, albeit much smaller influences of the morphology and texture cannot be ruled out at the moment. More detailed investigations on the stress, texture and supersaturation are necessary and will be carried out shortly.

### Acknowledgements

## References

[1] R. M. Bradley, J. M. E. Harper and D.A. Smith, J. Appl. Phys. 60 (1986) 4160.

[2] F.A. Smidt, Inter. Mater. Rev. 35 (1990) 61.

[3] J. Pelleg et al., Thin Solid Films 197 (1991) 117.

[4] G.N. Van Wyk, H.J. Smith, Nucl. Instr. Meth. A 170 (1980) 443.

[5] K.U. Kainer, Magnesium: Eigenschaften, Anwendungen, Potentiale, VCH, Weinheim, 2000, p.1.

[6] M. O. Pekguleryuz and A. A. Kaya, Adv. Eng. Mat. 5 (2003) 866.

[7] C. Potzies and K.U. Kainer, Adv. Eng. Mat. 6 (2004) 281.

[8] Z. Bin Sajuri, T. Umehara, Y. Miyashita and Y. Mutoh, Adv. Eng. Mat. 5 (2003) 910.

[9] G. Song and A. Atrens, Adv. Eng. Mat. 5 (2003) 837.

[10] A. Yamamoto A. Watanabe, K. Sugahara, H. Tsubakino, S. Fukumoto, Scripta Mater. 44 (2001) 1039.

[11] M. Zeuner, F. Scholze, H. Neumann, T. Chassé, G. Otto, D. Roth, A. Hellmich, B. O-cker, Surf. Coat. Techn. 142/144 (2001) 11.

[12] S. Mändl, Y. Bohne, J.W. Gerlach, W. Assmann, B. Rauschenbach, Nucl. Instrum. Meth. B 249 (2006) 297.

[13] J.A. Thornton, J. Vac. Sci. Technol. A 4 (1974) 666.

[14] I. Petrov, L. Hultman, U. Helmersson, J.-E. Sundgren, J.E. Greene, Thin Solid Films 169 (1989) 299.

[15] J. Bøttiger, J. Chevallier, J. H. Petersen, N. Schell, W. Matz, A. Mücklich, J. Appl. Phys. 91 (2002) 5429.

[16] D. Manova, W. Attenberger, S. Mändl, B. Stritzker, B. Rauschenbach, J. Vac. Sci. Technol. A 22 (2004) 2299.

Table 1: Deposition process parameters for the different PVD processes.

| | Magnetron Sputtering | Ion Beam Sputtering | IBS + Arc | Vacuum Arc |
|---|---|---|---|---|
| **Ion source/ targets** | 1 Magnetron Source: Mg + alloy targets | 1 Ion Source: Mg + alloys & composite targets | 2 Ion sources: alloy target + Ti cathode | 1 Ion Source: Mg or Ti cathode |
| **Process parameters** | Ar+ ions Power: 160 W Pressure : 0.2 Pa | Ar+ ions Energy: 0.8 – 1.2 kV Current: 30 – 34 mA | | Current: 100 A Voltage: 15 – 25 V |
| **Average Energy (eV)** | 5 – 10 | 8 – 15 | 10 – 25 | 15 – 45 |
| **Deposition Rate (µm/h)** | 3 – 5 | 1 – 3 (– 10) | 1 – 3 (– 10) | 1 – 3 (– 10) |

## Figure Captions

Fig. 1: Surface morphology of Mg films deposited by (a) MS, (b) IBS, and (c) VAD.

Fig. 2: XRD spectra of Mg-Sn alloys deposited by IBS at different compositions.

Fig. 3: Mg(101) polefigure of a Mg-Al-Zr alloy deposited by IBS.

Fig. 4: Polarization curves for different alloys. The transition from cathodic protection towards active dissolution is defined by the corrosion potential of cast Mg..
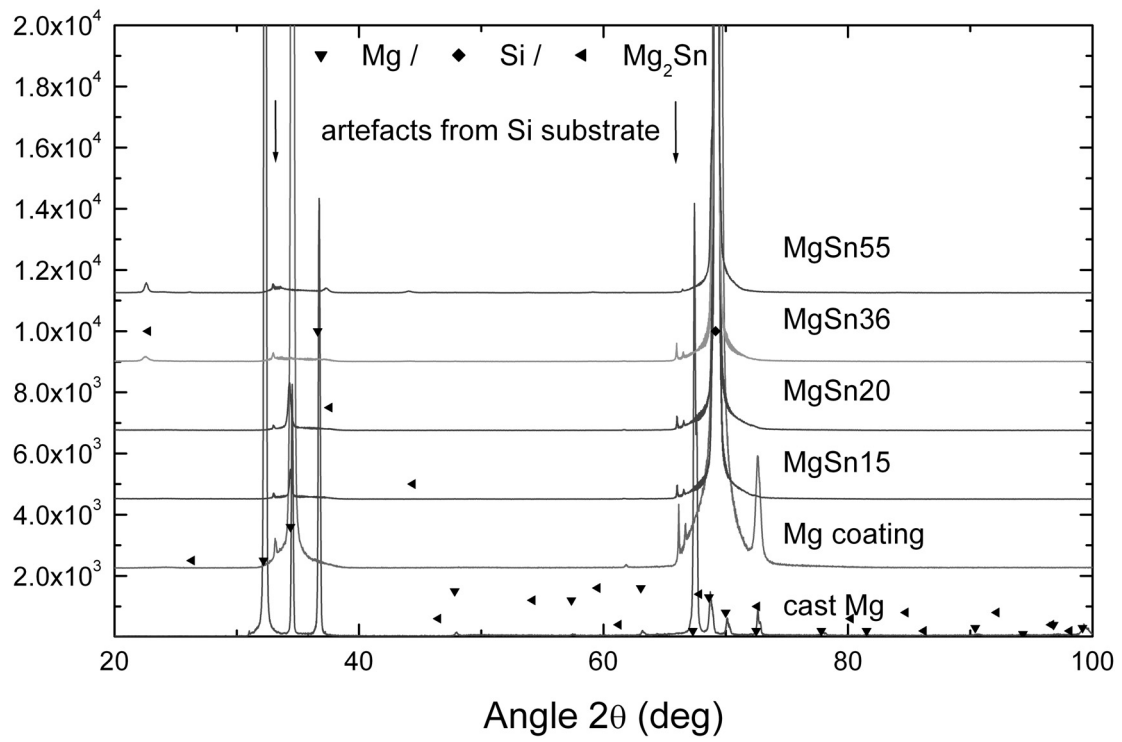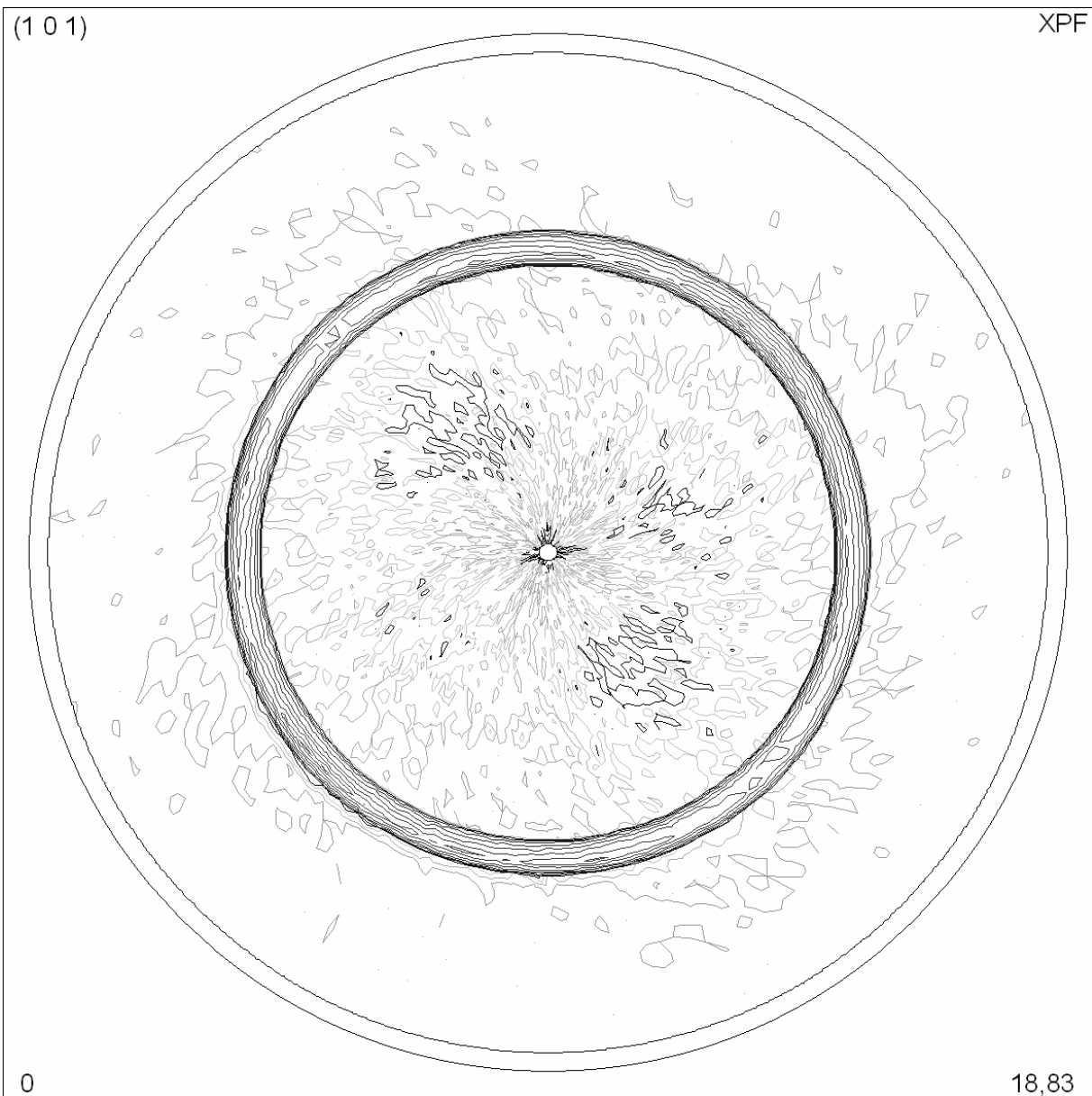
a)

b)

c)
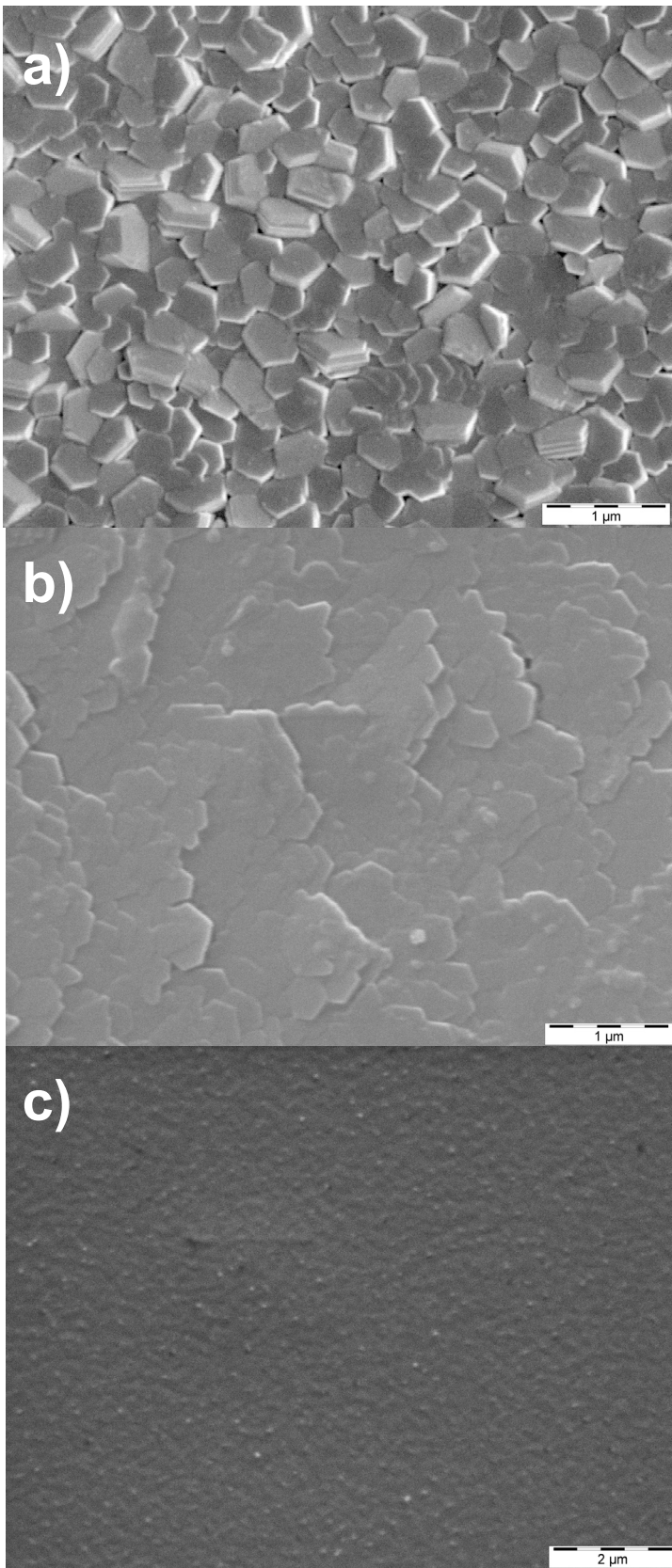
**Fig. 1**                    **Bohne et al.**

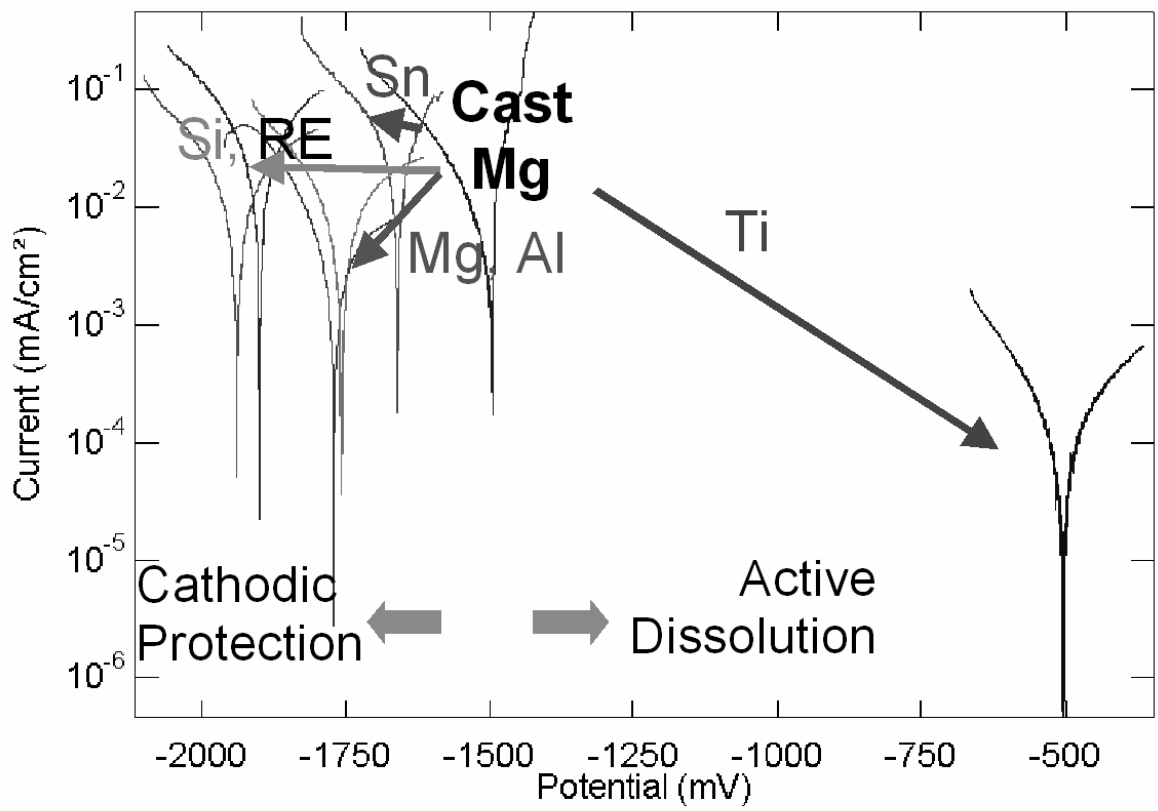**Fig. 2**                                 **Bohne et al.**

(1 0 1)  XPF

0  18,83

**Fig. 3**  **Bohne et al.**

**Fig. 4**                    **Bohne et al.**